TOPICAL REVIEW

A Comprehensive Review and Comparison of the Fragility Curves Used for Resilience Assessments in Power Systems

ALEXANDRE SERRANO-FONTOVA[1], (Student Member, IEEE),
HAIYU LI[1], (Senior Member, IEEE), **ZHIYU LIAO**[1], **MAGNUS RORY JAMIESON**[2],
ROSA SERRANO[1], (Student Member, IEEE),
ALESSANDRA PARISIO[1], (Senior Member, IEEE),
AND MATHAIOS PANTELI[3], (Senior Member, IEEE)

[1]The University of Manchester, M13 9PL Manchester, U.K.
[2]University of Strathclyde, G1 1XQ Glasgow, U.K.
[3]University of Cyprus, 1678 Nicosia, Cyprus

Corresponding author: Haiyu Li (haiyu.li@manchester.ac.uk)

ABSTRACT Over the years, power systems have been severely affected by extreme events. This situation has worsened given that climate change has proven to exacerbate their frequency and magnitude. In this context, resilience assessments have proved crucial to prevent and tackle the effects of these events on power systems. Some resilience studies have taken advantage of the so-called fragility curves (FCs) to evaluate the vulnerability of the system components against these natural hazards. Conceptually, FCs provide the failure probability of a particular grid asset according to the intensity of an extreme event, which can be determined based on the hazard intensity inherently dictated by the nature of the event. The probability of failure can be obtained following diverse methodologies and criteria. Thus, the resilience assessment of the event may vary significantly depending on how the probability of failure was determined. This paper provides, for the first time, a comprehensive review of the FCs used to model the vulnerability of the power system components, classifying them according to the physical magnitude and the system element subject to each type of event. Furthermore, a comparison of results obtained applying different FCs is developed to show the relevance of their modelling. The content of this paper can be used as a hands-on guide for researchers and power systems engineers to perform resilience studies.

INDEX TERMS Resilience, fragility curves (FCs), distribution networks (DNs), transmission networks (TNs), natural hazards, resilience assessments.

I. INTRODUCTION

In recent years, extreme weather-related events have notably risen and, unfortunately, become more frequent as an aftermath of climate change [1], [2], [3]. According to [4], natural hazards can be classified according to the following six categories: geophysical, hydrological, meteorological, climatological, biological, and extra-terrestrial. This research focuses on events belonging to the four first categories, dismissing those included in the last two. Geophysical hazards are inextricably linked to earthquakes and volcanic activity. Hydrological hazards are closely related to water movement and entail floods, landslides, and wave action. Meteorological events include storms, extreme temperatures, and fog. In the last instance, climatological events with greenhouse effects, including droughts and wildfires.

Power systems have been harshly affected by such natural hazards, where the security of supply is ultimately the major concern [5]. For instance, if windstorms are considered, several events have been reported to be severely damaging and

The associate editor coordinating the review of this manuscript and approving it for publication was Ali Raza.

causing significant disruptions worldwide, as indicated by the comprehensive report in [4]. For example, recent windstorms named Dudley, Eunice and Franklin hit the UK between 2021 and 2022, causing an estimated economic loss of £497 million, leaving 1.4 million households without power [6]. Similarly, hurricanes Harvey and Irma caused an estimated total economic loss of around $202 billion in the US [7]. Another example is the winter storm Uri, which hit Texas in February 2021. This storm led to large-scale generator outages and a load shedding of up to 25GW (equating to 33% of the total load), leaving 4.5 million customers without power during the most severe period (February 15th ∼ 16th) [8].

Tropical countries have recently reported a sudden increase in these extreme events, wherein strong wind gusts and severe flooding were recorded [9]. However, it is important to note that, in some cases, due to the accumulated precipitation, mudslides and ground movements can also occur along with strong wind gusts. On the other hand, helpful information regarding the severity of earthquakes can be found in [10]. The economic losses caused by this type of natural disaster are estimated to cost roughly $502 billion yearly [11]. As an example, an earthquake of 8.8 on the Richter scale hit the south-central area of Chile on February 27th, 2010, at 03:34 AM. The blackout due to the earthquake affected 4.5 million customers. The supply of eighty per cent of the customers located close to the epicentre was recovered approximately one week after the event. However, 0.4% of customers remained without supply two weeks after the event.

Wildfires also deserve special attention since they may pose a massive threat to power systems, as stems from [12]. From July 2017 to July 2018, a series of extreme wildfires devastated California, becoming the worst forest fire season in the history of California (USA). Fires have had overwhelming consequences, and it is estimated that they have caused about US$ 50 billion of economic loss, the bankruptcy of the local utility PG&E, and the destruction of 28,000 structures. The continuity of supply was also heavily affected, reaching 350,000 customers without supply in October 2017.

The significant impact of natural hazards on power systems is explained because the latter have been traditionally designed and operated under reliability criteria, meaning that power systems are able to work under normal or reasonable abnormal conditions but not to deal successfully with extreme events. Thus, it is necessary to include resilience criteria to improve the system response. The latest report carried out by the IEEE Task force on resilience defined the term resilience as ''The ability to limit the extent, system impact, and duration of degradation to sustain critical services following an extraordinary event. Key enablers for a resilient response include the capacity to anticipate, absorb, rapidly recover from, adapt to, and learn from such an event. Extraordinary events for the power system may be caused by natural threats, accidents, equipment failures, and deliberate physical or cyber-attacks'' [13]. As observed from the previous summary of reports, assessing resilience becomes
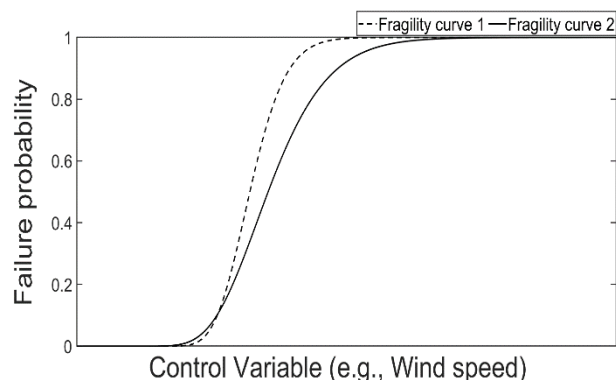

FIGURE 1. Generic shape of two different FCs.

crucial to prevent and minimise their impact on power system performance [14], [15], [16], [17], [18], [19], [20], [21], [22], [23], [24], [25], [26], [27], [28], [29], [30], [31], [32], [33], [34], [35], [36], [37], [38], [39], [40], [41].

To grapple with seismic events, the following studies have been published [26], [52], [53]. On the other hand, however, [15], [16], and [34], [36] are resilience-oriented approaches for extreme weather events, including windstorms, hurricanes, and typhoons. In [24], a comprehensive analysis has been conducted to cope with the effects of flooding in substations. Finally, the research in [40] and [41] delved into the impact of ice storms on electrical power systems.

It is vital to underscore, though, that regardless of the type of event analysed in each of the previously cited resilience-oriented articles, the use of fragility curves (FCs) is the guiding principle among them. According to Schulz et al. [43], from a conceptual point of view, FCs are functions that describe the probability of failure, conditioned on the load, over the full range of loads to which a system might be exposed. For example, the Federal Emergency Management Agency (FEMA) has taken advantage of real observations to develop FCs of critical infrastructure during natural hazards [42]. Further on, the types of curves encompassed in this reference are perused.

In this regard, FCs are indeed a handy tool to predict the vulnerability of the electrical grids against weather events. For instance, each weather-related event mentioned above implies a sudden rise of the associated inherent variables (e.g., high wind gusts during windstorms). Therefore, given this input as a variable, the probability of failure of an asset can be obtained, as can be seen in Fig. 1. It is worth stressing that not only one variable can be out of range during one of the previously cited events, as the electrical grid can be occasionally affected in several ways throughout the same event (e.g., high wind gusts combined with flooding). Given the need to enhance the resilience of the electrical grid, the authors believe that scrutinising how these FCs are obtained and how they impact the modelling of the vulnerability of system components can be highly beneficial to improve the accuracy of the resilience-oriented assessments and provide

a hands-on guide for grid planners and researchers. Moreover, the present paper is particularly of interest as any other research article has been previously published, where the FCs are reviewed and compared through numerical analysis.

The contributions of this paper are listed as follows:

- A comprehensive review of the existing FCs designed to model the vulnerability of power system components.
- A classification of FCs according to each type of natural hazard highlighting the main differences between FCs.
- Analysis of the most cited works to date and those that have not been yet cited, as are potential resources for future resilience-oriented assessments.
- Performing numerical simulations to underscore the impact on resilience assessments when relying on fragility curves.

The rest of this paper is structured as follows; Section II recalls the main types of resilience assessments. Section III elaborates on how the FCs are defined and obtained. The type of events for which the FCs have been designed are analysed in Section IV. A comparison between some curves is included in Section V. The analytical equations required to quantify the effects of the vulnerability models for wind events are perused in Section VI. Section VII discusses the influential factors of the FCs. Finally, Section VIII highlights the main advantages and challenges of the existing FCs.

II. TYPES OF RESILIENCE ASSESSMENTS

This Section recalls the main types of resilience assessments used in power systems where the FCs are commonly used as the main input.

Overall, the resilience assessments for power systems can be divided according to the timeline of the event (i.e., before, during and after the event), as discussed in the extensive report recently published in [13]. Several resilience reviews have also been published wherein different categorisations and definitions are illustrated [5], [44], [45], [46], [47], [48], [49], [50]. Nonetheless, this paper refers to the distinction provided by [13], where planning and operational assessments are defined.

A. PLANNING ASSESSMENTS

The resilience assessments focusing on the action before the event occurrence fall within the planning category, which, in turn, are further subdivided into the long-term and short-term (i.e., also known as preventive measures) [15], [16], [21], [27], [36], [37], [39], [40], [51].

Firstly, from a long-term planning standpoint, the assessments can be distinguished as hardening-based and software-based. Concretely, the hardening-based approaches essentially entail investing in new assets to make the grid bigger and, therefore, more robust (e.g., the rollout of new lines, substation equipment replacement and upgrade, trimming vegetation, promoting DERs engagement, etc.). On the contrary, software-based algorithms cover all aspects of automation and control. As an example, a mid-term approach

was carried out by Souto et al. in [34] for flooding, whereas [52], [53] et al. proposed a long-term power systems hardening strategy for earthquakes. The authors in [30] explored the feasibility of a software-based algorithm using grid automation and DERs to weather extreme events.

Secondly, within the short-term, the approaches considering a timeframe between a day and a few hours before the event are widely known as preventive and preparative [18], [21], [27], [36], [39], [40], [54], [55], [56]. For instance, [21], [36], and [56] have proposed day-ahead assessments to commit generation units and re-structure the grid considering extreme weather events. In line with these three studies, in [55], Lei et al. proposed to

B. OPERATIONAL ASSESSMENTS

As introduced earlier, evaluations designed to tackle the effects of an event that has already begun are known as operational resilience assessments. According to the categorisation in [13], these studies include early detection and emergency response plans as well as recovery strategies. When it comes to real-time detection, several studies have been published [14], [22], [38], [57], [58], [59], [60], [61], [62], [63], [64], [65]. In [2], the authors proposed a methodology to identify wildfires early and take further actions to avoid a major blackout. Liu et al. in [22] proposed a resilience-oriented approach wherein the fault location, fault isolation and restoration are jointly used along with distributed resources. Similarly, a proactive operation strategy to enhance system resilience during an ongoing extreme event is detailed in [35]. Finally, [58], [59], [60], [61], and [62] drilled down into the effects of cascading. It is worth noting that the common bottleneck of these techniques lies in implementing islanding operations to avert the cascading effects proactively.

III. ASPECTS OF THE FRAGILITY CURVES

As introduced in Section I, fragility curves are used to relate the failure probabilities of a component given the intensity of the physical magnitude during an event, expressed by means of its physical magnitude [43] (i.e., the physical magnitude used in the FCs). These curves are used to pinpoint the vulnerable assets of the grid (i.e., lines, substations, etc.), which constitute the first aspect in the majority of resilience assessments. Therefore, they can significantly influence the outcomes of such assessments. The following subsections describe the features of these curves, how they can be obtained, and the physical magnitudes used thus far in resilience assessments.

A. FRAGILITY CURVES: THE CONCEPT

The shape of a fragility curve describes the uncertainty in the capacity of the system to withstand specific events or loads. If there is little uncertainty in capacity or demand, the fragility curve will take the form of a step function, then having only two stages (i.e., 0 and 1 for non-faulted and faulted, respectively). On the contrary, as seen in many recent fragility studies [68], it is assumed that the FCs follow a

lognormal distribution and can be described by the cumulative distribution function as in (1)

$$f(x) = \frac{l}{\sigma\sqrt{2\pi}} e^{-\frac{1}{2}\left(\frac{x-\mu}{\sigma}\right)^2} \tag{1}$$

where x is a normally distributed variable and is represented by the hazard intensity used in each type of FC (e.g., wind speed in windstorms), μ and σ are the mean and variance, respectively. The FCs also stem from the reliability indices expressed through the conditional failure probability. Hence, depending on μ and σ, the slope of the FC will vary and, consequently, the probability of failure. To illustrate the differences between FCs, two curves with different parameters are displayed in Fig. 1.

## B. TECHNIQUES TO OBTAIN THE FRAGILITY CURVES

According to the distinction in [43], the methodology used to derive the FCs can be divided according to four main typologies: (i) judgmental, (ii) empirical, (iii) analytical, and ultimately, (iv) hybrid.

Judgmental methods build FCs based on experience, which is not limited by the quantity and quality of available data but may be subject to bias caused by personal experience. For example, the FCs obtained using expert criteria are used in [67] and were obtained from studies carried out by the Mazandaran power distribution company in Iran.

Empirical methods are based on field and/or lab measurements to model the performance of the components. However, those observations may be systematically obtained through controlled experiments or collected opportunistically, which adds uncertainty to the model. An advantage of using these techniques is that interactions between the structure of the element object of study and the environment can be deemed [68], [69], [70].

FCs obtained through analytical methods have been widely used in recent years as they can be performed by taking advantage of purely analytical or numerical techniques [71], [72], [73], [74]. Moreover, within the previously mentioned numerical techniques, the stochastic approaches have played a pivotal role in accounting for uncertainty [75]. An emerging trend to design FCs combining both judgmental and analytical techniques using machine learning is gaining momentum [68]. In the last instance, combining two or more of the methods described above leads to the so-called hybrid methods. For example, these hybrid methods for FCs can be implemented by using an empirical approach over a certain range of values of the hazard intensity, whilst an analytical one is used for the rest of the values [72].

Additionally, it is worth saying that the main difference between empirical and analytical is that empirical-based FCs are, to a certain extent, limited to the asset object of study and its environment, being difficult to be extrapolated and consider additional factors. On the contrary, however, analytical curves can consider additional factors and/or explore the interaction between the asset and other factors.
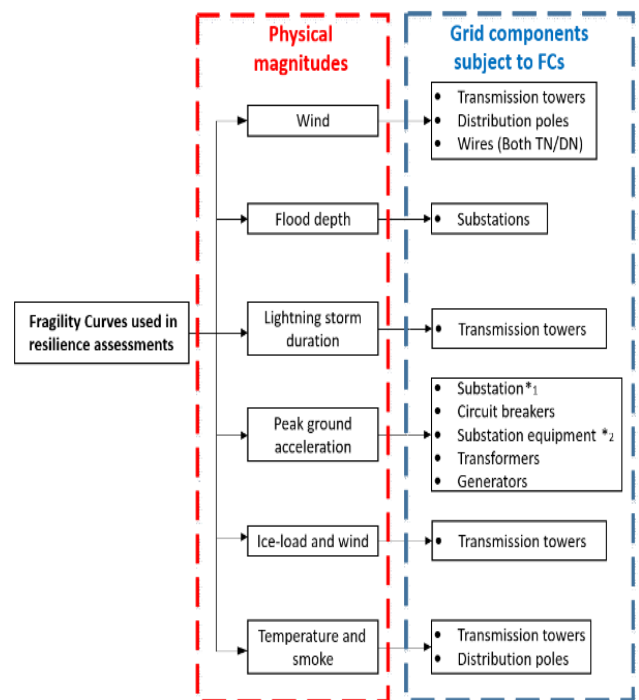
FIGURE 2. Main types of magnitudes and components considered in the FCs for resilience assessments. *1 Substation as a sole component; *2 Protective devices within a substation.

IV. FRAGILITY CURVES ACCORDING TO EACH NATURAL HAZARD

Fig. 2 illustrates the relationship between the typical physical magnitudes used in modelling FCs and the grid components affected. It is worth mentioning that although a large part of studies has only considered one input variable to develop the FCs (e.g., those in [74]), some others have included several magnitudes, resulting in multi-dimensional plots (see, for example, [75]). The electrical grid components whose vulnerability is subject to FCs are included in the blue square.

A. WIND-BASED FRAGILITY CURVES

This subsection covers the FCs designed for components exposed to wind hazards, such as towers and lines. Given the fact that transmission and distribution systems are composed of elements with different materials and structures, the FCs have been divided according to that distinction.

1) FRAGILITY CURVES FOR TRANSMISSION SYSTEMS

The focal point of [68], [69], [70], [75], [76], [77], [78], [79], and [80] lies in developing FCs curves for transmission lines against wind hazards. In [68], the authors delved into a spatiotemporal approach to ascribe likely failures during severe windstorms. To generate empirical FCs for electrical overhead lines, a dataset of over 12,000 electrical failures was correlated to a windstorm model based on the European reanalysis meteorological agency. Similarly, studies [69], [70] use field measurements to develop the FCs, thus being empirical-based approaches. These two works provided FCs

for 132 kV and 220 kV transmission lines based on observations obtained in the transmission systems in Scotland (UK).

A probabilistic analysis framework for achieving a lifetime multi-hazard fragility model has been deemed by C. Li et al. in [75]. This method provides the FCs of a multi-hazard where the simultaneous occurrence of peak-ground acceleration and wind is considered. On the other hand, the authors in [76] explored the feasibility of FCs for transmission towers by conducting static non-linear buckling analysis where both the wind speed and angle attack are considered. The analysis in [76] also points out the influence of uncertainties regarding material properties and Section dimensions when developing FCs. The authors in [77] have investigated the vulnerability of transmission towers exposed to heavy rain and wind gusts simultaneously. The equivalent basic wind speed is used to model the vulnerability of the transmission towers. To date, this approach is the first to shed some light on the effects of multi-hazards on both hurricanes and typhoons. A novel concept, however, is defined in a recent study conducted by Hou et al. [78], where the behaviour of fallen trees in power lines was first introduced. To that end, the finite element modelling of the trees subjected to wind loads is performed based on the fragility curves of several typical urban tree species. Besides the probability of failure, this study also provides the analytical equations to calculate the critical distance to avert the crash of fallen trees into overhead power lines.

The outcomes of the research study in [79] underscore the importance of neglecting the relationship line-tower in fragility studies, which is an assumption made by the previously cited studies. This paper has used an explicit integration method to analyse the dynamic response of the transmission tower-line system under intensive wind loads. A comparison between models with and without considering such a dependency is perused in this paper.

Eventually, unlike the previous works, the authors in [80] have strived to model the vulnerability of the conductors in transmission lines. Crucially, a sensitivity analysis accounting for various types of wires and span lengths is used as a proof-of-concept for some FCs. It is worth saying, though, that the curves developed in [80] could be used in conjunction with any of the above-cited articles designed for transmission

2) FRAGILITY CURVES FOR DISTRIBUTION SYSTEMS

The authors in [72] propose a Bayesian network to quantify the time-dependent nature of power distribution systems against hurricanes. To capture the failure probabilities of the poles within the power distribution system, fragility curves for the poles were generated through physics-based fragility analysis, incorporating properties of the pole-wire components and the pole-wire system topology. In [73] and [74], several FCs are obtained considering different classes of wood poles, including deterioration. In this direction, Vitaly et al. in [73] provided the analytical expressions and their associated parameters to compute the fragility curves based on each class type, the age of the pole, pole height, wind direction and conductor area.

S. Lee et al. have taken a step further in [81], where the FCs have been obtained for leaned wood poles. To analyse the moment behaviour of leaning poles, a new probabilistic framework for computing three types of loads by wind pressure has been suggested where the overturning force and conductor tension are also deemed. Thus, a set of FCs for utility poles with given ages and leaning angles are presented to assess the impact of leaning on the probability of failure. The vulnerability of steel-made poles has been explored in [82], where the framework includes a life-cycle cost analysis. To validate the dependability of the proposed methodology, field measurements have also been used. In [83], the resilience of the pole-wire system was analysed after establishing a system analysis framework to enhance the structural reliability by using hardening/inspection priority analysis based on Monte Carlo simulations. This study considers class three and class five poles with a height of 14 m and a span length of 61 m. Based on the discussion included in [83], the obtained set of FCs can provide the failure rate only for a single pole or a small pole group, but it cannot provide an overall pole failure rate for mixed poles and spans.

Hitherto, the previously described articles in this subsection considered only the fragility of the poles, disregarding the effects that one pole can cause on the adjacent ones. According to recent observations in the UK, this casuistry has also been neglected in transmission networks, but it may have sense, as it has proven to be a very rare and unusual event with large spans [28]. Nonetheless, this may not be the case in distribution networks, as the spans between poles could be much smaller than those in transmission networks. Thereby, [84] examined the effects of this factor on the reliability of power distribution lines against hurricanes. The couplings in the wind performance of adjacent spans are properly incorporated through an equivalent boundary model. Furthermore, the findings in [82] prove that the common assumption of independent failure events in poles used in distribution lines represents the worst-case scenario.

B. FRAGILITY CURVES FOR SEISMIC EVENTS

The intensity indicators used to measure the impact of these events include peak ground acceleration (PGA), peak ground velocity (PGV), peak ground displacement (PGD), and spectral acceleration at the fundamental frequency of the concerned structure (Sa). Although most FCs are given according to the PGA or the Sa, some earthquake studies further classified the threat according to near-field and far-field, respectively [86]. The components of the electrical power systems subject to earthquakes are the following:

1. Towers (either distribution or transmission) [85], [87], [88]
2. Generation units [85], [86], [89], [90]
3. Transformers [85], [91], [92], [93]

4. Substations [85], [94]

5. Protective devices [92], [94], [95]

The vulnerability of distribution poles due to earthquakes is the object of study of [85]. It must be noted that the vulnerability is computed with respect to the total amount of lines in the feeder instead of pinning down each line or Section of the grid. In this sense, four damage states have been comprised (i.e., slight, moderate, extensive and complete), where the percentage of failure with respect to the total number of lines is 4%, 12%, 50% and 80%, respectively. In [87], some FCs have been developed for concrete-made poles in power distribution networks. To fulfil that purpose, the H-type reinforced model of the concrete pole was developed and verified using past experimental studies as well as the observed damage in previous earthquakes. Since this technique has combined real observations with numerical simulation studies, it can be considered a hybrid approach. Nevertheless, the researchers in [84] focused on the effects of earthquakes on the transmission towers. If the outcomes of both studies are assessed, relevant differences are observed. In addition to these two studies, a set of FCs are obtained for distribution systems, including poles and wires, wherein both overhead and underground types and in-line equipment are included [85]. In [85], the FCs provide a certain percentage of unavailability with respect to the total number of lines in a feeder instead of locally assessing each asset.

The second typology listed in the previous categorisation is power generation units. It covers a wide range of cases according to each main energy source, leading to different casuistries. In [85], [87], and [88], a distinction was made between small and large power plants, where 100 MW is the threshold for that case. The provided FCs rely on the degree of damage experienced by the power station, where four statuses are deemed; slight, moderate, extensive and complete. Hence, all types of power plants are encompassed within this category regardless of the designed infrastructure and nature of their prime source. Despite being a helpful guide, a more detailed approach would perhaps be required if the resilience assessment addresses a particular type of generation unit. For example, Zhao et al. in [86] investigated the effects of earthquakes in nuclear power plants where a set of FCs are obtained. Specifically, [86] designed FCs for auxiliary and shield-building equipment.

In addition, a detailed vulnerability model of a diesel generator during earthquakes has been undertaken in [89]. In it, the FCs of the internal pieces are combined to obtain a final FC for the generator itself. D. Ngo et al. have dug into the seismic structural response of wind turbines and proposed a novel solution [90]. The need to investigate the vulnerability of power transformers has been gaining increased prominence recently, given the fact that they are a key element in power systems. The power transformer was included as a part of the substation in [85], but there are no specific FCs for it. On the contrary, the vulnerability of transformers against earthquakes has been investigated in [91], where several FCs are obtained. This technique used the dynamic characteristics

of the analytical model. Differently, the main pillar of the research conducted in [93] provided features to obtain FCs yet is purely supported by field measurements. In such a study, a large database extracted from events recorded in the USA was included to obtain such FCs.

At the time of writing, the fragility of electrical substations has been addressed from two different pathways. The first considers the substation as one sole element and establishes four stages of damage, where each one is associated with a failure percentage of the disconnect switches and circuit breakers in the substation [85]. This model, nonetheless, does not stand for the fragility modelling of each element within the substation. To that end, the authors in [94] first introduced the vulnerability of each element embedded in the substation, such as disconnection switches, circuit breakers, current and potential transformers and lightning arresters. The extensive report included in [94], provides failure rates based on real measurements where the elements in substations are classified according to the voltage level. The last research assessment can be likened to the one in [92] as it individually pinpoints each element within a substation. The approach in [92] has slightly broadened that topic as it provided the required parameters to construct the FCs and intertwined such features with the seismic activity of the earth. In this case, only 110 kV substations were taken into consideration. In addition to the FCs for protective devices provided in [94] and [92], Paolacci et al. in [96] assessed the fragility modelling of vertical high-voltage disconnectors. It must be said that the model included in [92] was achieved by combining the standard reliability methods for time-invariant problems with the response surface technique. The proposed technique permits the development of FCs using a very limited number of numerical simulations.

C. ICE LOAD AND WIND FRAGILITY MODELS

This Section examines the works carried out to model the effects of ice storms on the electrical systems infrastructure. This type of event is understood to cause high precipitation along with strong winds. Since the collapse of an electrical tower can be determined by the mechanical stress as indicated in [97], the ice accretion seems to be a reliable indicator for vulnerability analysis in resilience studies see, for example, [41], [98], and [99]. A thorough dissertation regarding the techniques used to calculate ice accretion is provided in [100]. In this direction, Yang et al. exhibited successful results in predicting the freezing fraction and collision coefficient parameters of the ice accretion [101]. In [102], the effects of wind and ice loads on transmission towers are presented. The reliability calculation is based on a Monte-Carlo technique where each scenario represents a certain weather situation. The model considers the speed of the storm as the main input to obtain the distance to the electrical conductors, where the radius of the storm is the critical parameter. Since the fragility of transmission lines depends on the accumulated weight, the risk of failure, in turn, depends on both the weight and

duration of the ice storm. Similarly, the authors in [102] provided a 2-D approach where wind and ice thickness represent the axis and, resultingly, four regions can be identified. Each region stands for a different level of risk. Subsequently, the vulnerability of towers can be obtained, whether it is because of high winds, low ice thickness, or a combination of both. On the other hand, given that the ice thickness is a reliable magnitude to estimate the load on towers, the resilience assessment in [41] relied on a piece-wise function where a synthetic ice-wind load is the input variable.

The research outcomes published in [103] underline the robustness of concrete poles and metal towers for combined wind and ice loads. The time-dependent performance processes of system elements are presented in terms of their random safety margin sequences. The survival probability of poles and towers as auto-systems representing their multi-criteria failure mode is discussed. The analytical equations and parameters to compute the FCs are provided for both wind and ice loads.

D. FLOOD-DEPTH-BASED FRAGILITY CURVES

The percentage of damage to power generation stations and substations has been developed in [42], with flood depth as the main input. The FCs using the flood depth that occurred in natural hazards are discussed in this subsection. However, it is worth pointing out that this model considers power generation plants and substations as one element, neglecting the effect of flooding in each included component. In addition to it, all types of generation plants are included in this model, disregarding the particularities of each typology.

Contrarily, the authors in [104] focused on elaborating curves for the secondary distribution centres, where the original curves proposed in [85] have been honed with real occurred events in the cities of Barcelona and Bristol. This approach took advantage of a spatiotemporal representation of the low-voltage distribution centres in those two cities. Even though it has not focused entirely on the electrical facilities, the study in [105] has certainly derived a family of FCs. This model includes a single-storey structure made of timber, masonry and concrete with five stages of damage. This research also presents a method to retrieve the mean damage curves from other FCs obtained in the literature, using cost coefficients associated with each of the four damage states.

E. FRAGILITY CURVES USED FOR WILDFIRES

According to [106], the most noticeable indicator regarding the impact of wildfires on electrical lines typically lies in the thermal stress experienced by the electrical wires. In such circumstances, the capacity of the conductor can be indirectly influenced by the heat and smoke, even if there is no severe damage to the utility towers. Therefore, instead of a fragility curve as such, the authors in [107] provided the analytical expressions required to calculate the acceptable safety distance between the fire and the target line. In this model, the

flame is considered a geometrical body that emits radiative heat uniformly throughout its entire surface area, and the wind speed is omitted. Choobineh et al. expanded the previous model and incorporated the wind speed in [108] by using the solid flame model to predict fire advance in a detailed geometrical representation. The model developed in [108] was previously used in [109], [110], [111], and [112] to lessen the effects of wildfires and enhance resilience. A significant contribution towards an early warning against wildfires has been carried out in [2], where the proposed model simulates a spatiotemporal representation of the wildfire via a geography cellular automata model, which is able to predict when and where the wildfires are likely to reach the transmission line. Additionally, both a line outage model and a FC are proposed based on the wildfire prediction and breakdown mechanisms. The two-dimensional FC gives the probability of failure given the temperature of the conductors and smoke density as input variables.

F. FRAGILITY CURVES BASED ON LIGHTNING DURATION

The focal point of this subsection is the analysis of the FCs and vulnerability models developed for the electrical power system elements during lightning storms. To measure the effects of lightning on the electrical towers, the authors in [113] coined a new definition that includes the location, the current of the strike, and the number of times the lightning movement track crosses a particular transmission line. Further on, the same authors proposed in [17] a few FCs to compute the failure probabilities of each line, where the input variable is the duration of the storm. The implemented lightning location system proved quite successful for real-time lightning vulnerability prediction.

Murray has studied a different approach where lightning storms have been retrieved from real measurements in Scotland [17]. In addition to the previously mentioned works, as part of the PhD in [114], the convective available potential energy has been put forward as a novel indicator, yet any FC has been derived.

G. SUMMARY OF THE EVALUATED FCs

A general classification is provided in this Section to give the reader a clear understanding of the types of FCs and the main typologies. In a nutshell, Fig. 3(a) displays the total number of articles where the FCs are the object of study. From that chart, it seems clear that wind-based FCs are the most explored ones. In contrast, the vulnerability of the grid against flooding and ice storms is still a matter of future research.

On the other hand, Fig. 3(b) shows the trend regarding FCs, where the increase in recent years is quite noticeable, showing the relevance of this concept for resilience assessments. In addition to the previous distinction, Fig. 4 illustrates how those FCs are intertwined with resilience assessments. Finally, Table 1 provides a summary of the FCs according to the type of natural hazard. The present study shows that the most used FCs for wind in transmission networks are the ones
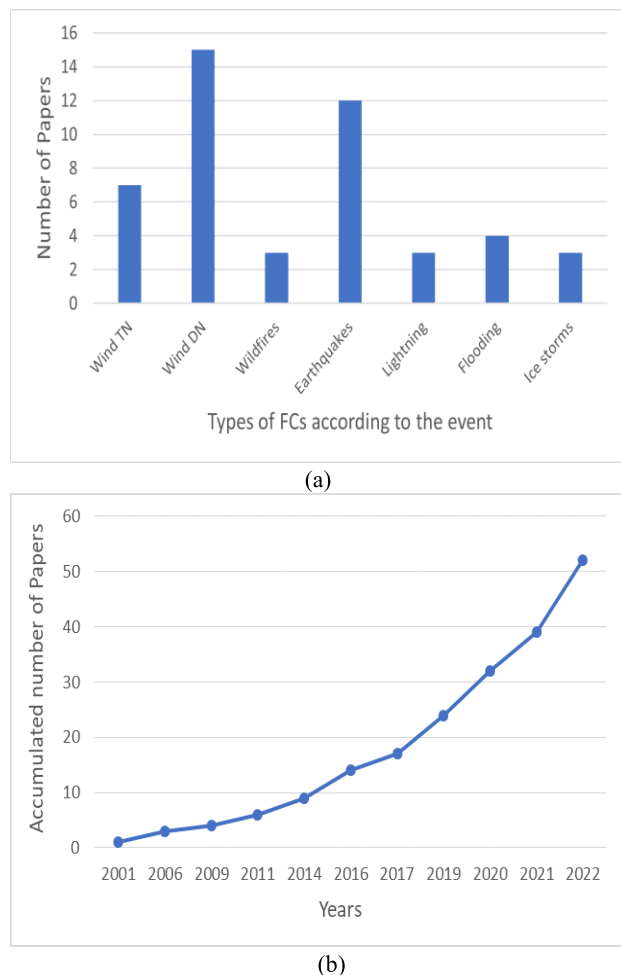
(a)

(b)

FIGURE 3. Trend of the published articles with FCs.

in [76], whereas those obtained from [74] are the most used for distribution networks.

Regarding earthquakes, it has been found that the most used curves are those implemented by FEMA [85]. For flooding events, the vast majority of resilience assessments chose the FC included in [42]. In addition, this research shows that the majority of studies use the radiative heat model proposed in [107] to determine the vulnerability of lines due to excessive heat transfer.

V. COMPARISON BETWEEN FRAGILITY CURVES

This Section provides a detailed comparison between the FCs used for a given test system component and physical magnitude so as to lay the ground for the numerical examples included in Section VI. Note that such a comparison can only be fulfilled for windstorms, as are those categories where several FCs are available for the same asset.

A. COMPARISON BETWEEN WIND-BASED FCs

Since the vulnerability of the system components is slightly different between transmission and distribution, as indicated in [115], this Section has divided the discussion into two main parts.

1) FRAGILITY CURVES FOR TRANSMISSION SYSTEMS

The fragility curves developed by means of either empirical or analytical tools to model the vulnerability of transmission systems are briefly compared in this Section.

Firstly, the performance of two sets of analytically obtained FCs are compared in Fig. 5. The study carried out by Xing. F et al. modelled a steel-made 500 kV-type transmission tower with a height of 99 m. The technical detail of the procedure to design such infrastructure can be found in [116]. In [76], a bilinear isotropic hardening plasticity model was simulated for steel towers. However, that article did not consider the interaction between the towers and the wires. Contrarily, the authors of [79] advocated investigating such a dependence. It must be stressed that although the height of the tower explored in [79] is 32 m and is above the one in [76], it is assumed that the 10-m wind value obtained from measurements has been scaled up to such a height in both studies and consequently a comparison can be safely be made. As can be drawn from the curves plotted in Fig. 5, the failure probability of the curves for each wind attack angle coincides in order of magnitude between references, but the tower-line interaction implies differences in the shape of the FCs. For example, there is a difference of 0.26 in the probability of failure between those curves for a given wind speed of 35 m/s impacting the transmission tower with an angle of 45 degrees. On the other hand, it is seen that for some points of operation, both curves offer the same level of robustness (e.g., 27 m/s, 30 m/s, 35 m/s for incidence angles of 90 deg., 60 deg. And 45 deg., respectively).

Secondly, the empirical FCs used to obtain the probabilities of failure of transmission lines in [70] and originally retrieved from [69] are scrutinised here. A distinction was made between lines operating at 132 kV and 220 kV, and 400 kV, accounting for different types of towers and mechanical features. The experimentally obtained failure rates retrieved from [70] are shown in Fig.6. It is worth noting that the failure probabilities displayed in Fig. 6 are based on either a 132kV or 275 kV-type line for every 100 km, where the 400 kV lines have been included in the 275 kV-type curve as their performance have been regarded to be fairly similar based on the field experience in the UK.

The empirical FCs used in [28], [59], [62], [63], [64], [65], and [117] have been retrieved from [118] as part of the RESNET project. These FCs are plotted in Fig. 7 and classified according to three degrees of vulnerability (i.e., base and +/− 20 % of robustness). The main difference between the empirical curves in [59] and [70] is that those in [70] output the vulnerability of towers and conductors separately, whereas the line is considered as a sole element in [59]. A discussion regarding the implications of assuming the previous criterion is detailed in Section III.

2) FRAGILITY CURVES FOR DISTRIBUTION SYSTEMS

Even though the types of distribution systems slightly differ depending on the country and voltage level, in this paper,
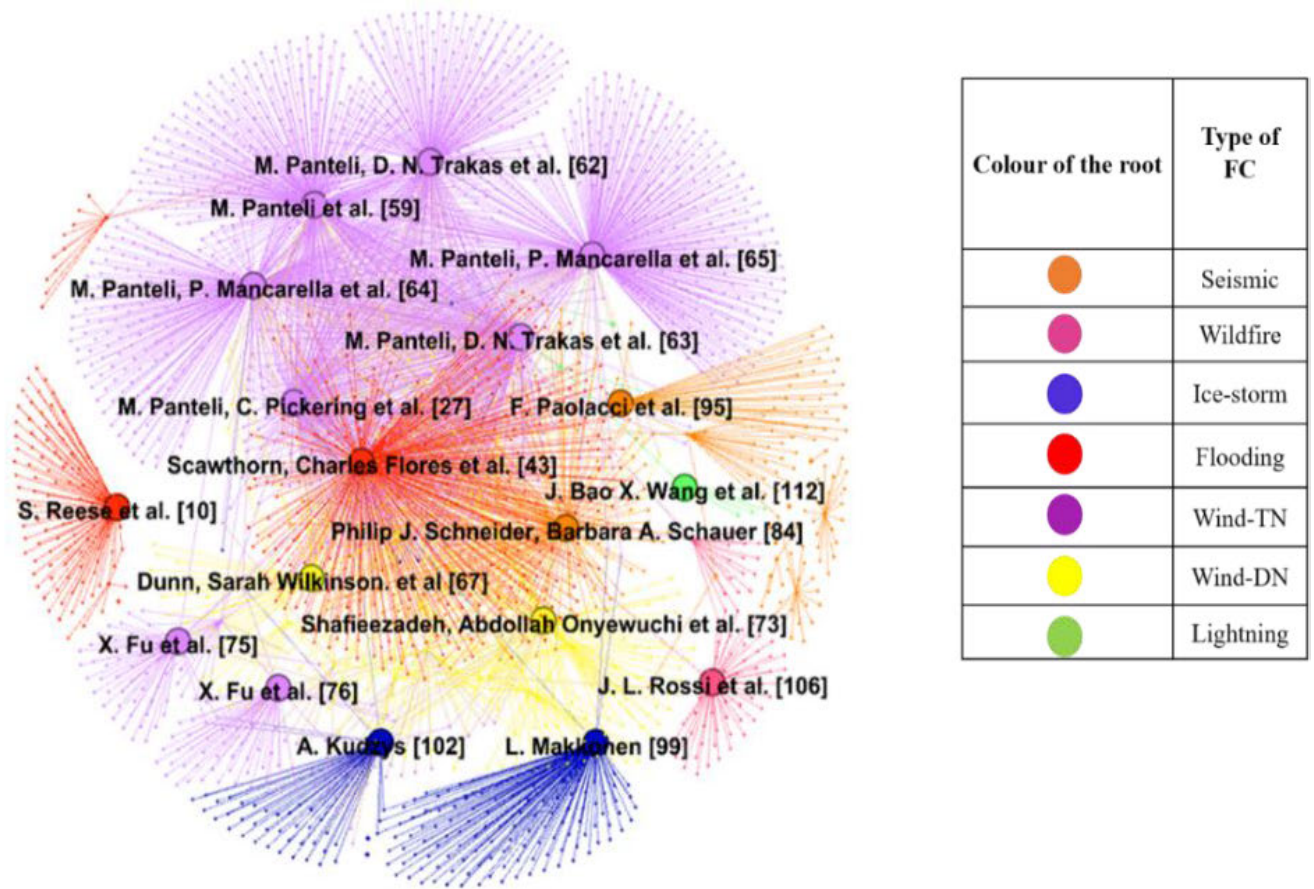
Colour of the root	Type of FC
🟠	Seismic
🟣	Wildfire
🔵	Ice-storm
🔴	Flooding
🟣	Wind-TN
🟡	Wind-DN
🟢	Lightning

FIGURE 4. Graphical representation of the FCs and their associated references covered in Section V.
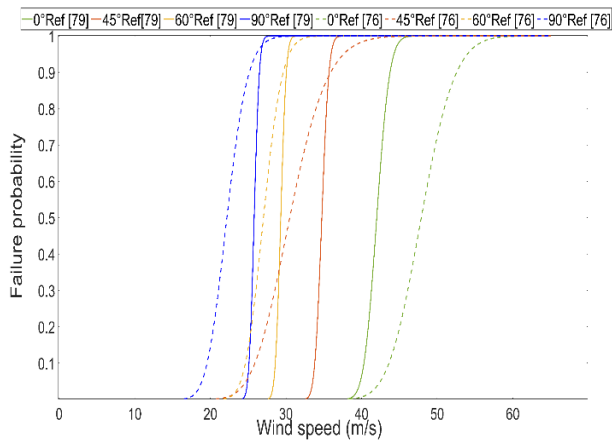

FIGURE 5. Comparison between the FCs in references [76] and [79].
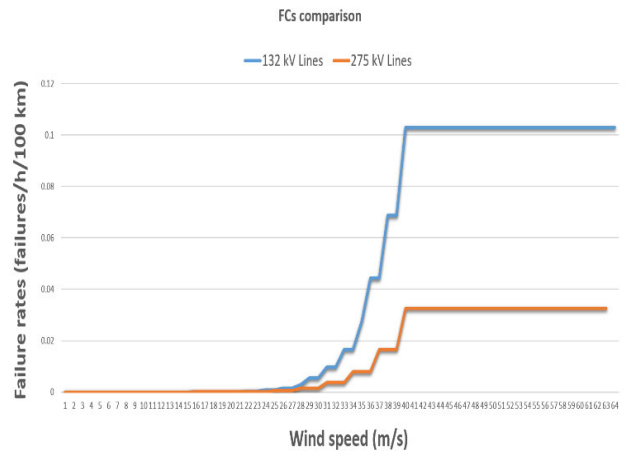

FIGURE 6. Empirical FCs obtained from [70].

any test system component operating below 132 kV has been regarded as distribution. Primarily, poles and wires are the most affected assets of the grid under wind load. A variety of classes and raw materials are commonly employed in DNs, see each type and their main features in [82]. For comparison purposes, the curves developed in [73], [74], and [81] for

Class five wood poles considering both new and 50-year-old ones are analysed in this subsection. The FCs of these references can be compared as the features in terms of pole height, pole class, material, and conductors' area (i.e., the number of conductors, cross-section and span length) are

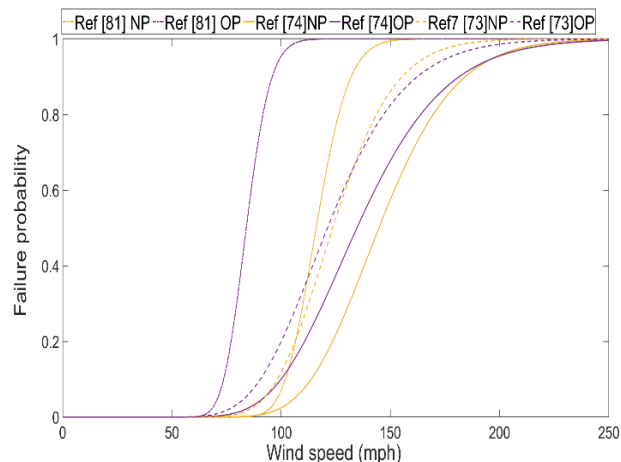**TABLE 1.** Types of fragility curves according to each natural hazard.

Type of Natural hazard	Asset of the grid	References
Windstorms and hurricanes	DN-Wood poles	[68, 73, 74, 81-84]
	DN-Wood and steel poles	[82]
	DN-Steel poles	[51]
	TN-Towers	[59, 69, 70, 75, 76, 79]
	TN-Poles and wires	[80]
Seismic events (Earthquakes)	Towers (TN and DN)	[85, 87, 88]
	Generators	[85, 86, 89, 90]
	Substations	[85, 94]
	Protective devices	[92, 94, 95]
Ice storms	Lines	[99-102]
Flooding	Substations, lines and generators	[42]
Wildfires	Lines (Transmission)	[2, 106]
Lightning	Lines (Transmission)	[113]
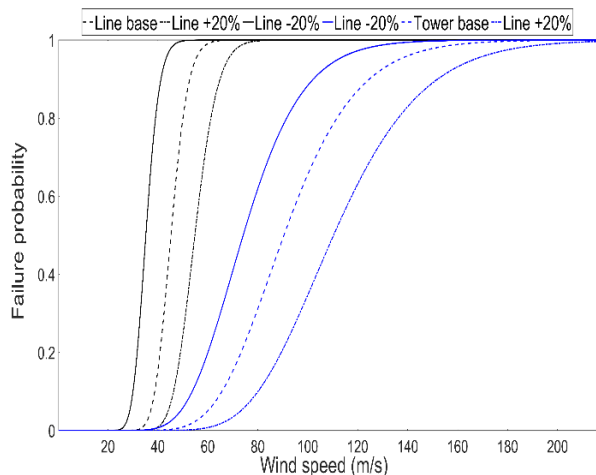
FIGURE 7. FCs provided in [59].

FIGURE 8. Comparison between the FCs in references [73], [74], [81].

relatively similar. The performance of new and aged poles for each reference is shown in Fig. 8. The pole height and span length were modelled with the mean and standard deviation in [74], being 11.4/1.0 m and 43.9/11.2 for both the height and span length, respectively. Darestani et al. provided the analytical equations of the FCs given a range of parameters and uncertainty [73]. In this paper, exactly the same parameters included in [74] have been considered with the equations in [73]. Similarly, an 11-m height Class 5 wood-type pole with an average span of 63.2 m was considered in [81].

It is worth underscoring that in [81], for the first time, the FCs modelled the deterioration of the pole in terms of bending. As an example to illustrate the differences between

curves, given those in Fig. 8 and considering a 3-s wind gust of 100 mph, the values obtained are 0.02, 0.08, and 0.12, for [73], [74], and [81], respectively. On the other hand, when it comes to old poles, given the same wind speed gust and references used above, the probabilities of failure are 0.1, 0.2, and 0.9, respectively. Please note that subscripts NP and OP stand for new and old poles, respectively.

VI. EFFECTS OF THE VULNERABILITY MODELLING ON RESILIENCE ASSESSMENTS

This Section delves into the effects of the previously compared FCs on the resilience assessments separately for each type of event and affected test system component.

A. RESILIENCE ASSESSMENTS FOR WIND EVENTS

1) ANALYTICAL EQUATIONS TO COMPUTE THE PROBABILITIES OF FAILURE

The failure of a line occurs due to either a tower collapse or wire breakage and is computed through equation (2). Hence, if the interaction between consecutive towers is neglected, the probability of failure of the ij line at each time t is as follows

$$P_{ij,t}^{L} = P_{ij,t}^{P} + P_{ij,t}^{B} - P_{ij,t}^{P}P_{ij,t}^{B}, \forall(ij) \in \Omega_L \forall t \in T \quad (2)$$

where $P_{ij,t}^{P}$ and $P_{ij,t}^{B}$ are the probability of failure of the $ijth$ line because of the pole and wire breakage, respectively. Moreover, Ω_L and T stand for the set of lines in the test system under investigation and the timeframe of the assessment, respectively. The probability that a line trips because of a tower collapse is given by (3) if all poles are exposed to the same conditions and therefore, the same FC suffices to model the vulnerability.

$$P_{ij,t}^{P} = 1 - \prod_{k=0}^{N_{ij}^{Poles}} (1 - P_{k,ij,t}), \forall(ij) \in \Omega_L \forall t \in T \quad (3)$$

where $P_{k,ij,t}$ is the probability of failure of the kth pole in each ij line obtained from the FCs and N_{ij}^{Poles} is the number of poles in each ij line. On the other hand, if a line is composed of electrical towers in several areas, the wind attack angle and speed may vary, and so may the probability of failure. In such a case, the probabilities are computed as in (4)

$$P_{ij,t}^{P} = 1 - \prod_{s=0}^{N_{ij}^{S}} (1 - P_{s,ij,t}), \forall(ij) \in \Omega_L \forall t \in T \quad (4)$$

where $P_{ij,t}$ is the failure probability of the $ijth$ line at time t and $P_{s,ij,t}$ the failure probability of each portion of the line in the sth region (i.e., the portion of each line crossing an area), which is obtained through (5)

$$P_{s,ij,t}^{P} = 1 - \prod_{k=0}^{N_{ij}^{S}} (1 - P_{k,s,ij,t}),$$
$$\forall(k) \in \Omega_{s,ij} \forall(ij) \in \Omega_L \forall t \in T \quad (5)$$

where $P_{k,s,ij,t}^{P}$ is the probability of failure of the towers in the $ijth$ line within the sth area at time t. This probability of failure applies for each gridded area, which may imply using different FCs because if the line disposition changes, so do the wind attack angle and speed.

2) TRANSMISSION SYSTEMS

The vulnerability of transmission lines against events involving strong winds is inextricably linked with the type of curve, as pointed out in Section V. Thereby, this Section aims to provide a quantitative analysis of these differences between models and their impact on the resilience assessments in terms of vulnerable lines.

Having said all the above, a high-resolution spatial model has been implemented by dividing the UK map into gridded
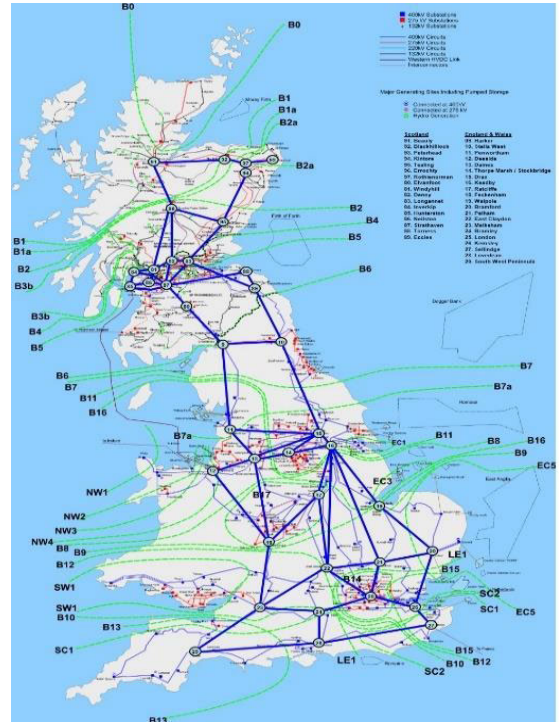
FIGURE 9. Reduced version of the GB Transmission system used in Section A-VI.2.

areas of 0.5 by 0.5 degrees of longitude and latitude, resulting in 288 areas. After that, the reduced 62-line 28-bus GB test system is mapped into the spatial model, as can be seen in Fig. 9. The GB model was obtained from [119]. Given that transmission lines may cross different areas, consequently subject to different wind speeds and attack angles, it was assumed that no significant wind speed and angle variations occur within each area, which is in line with the assumption made in [28]. The wind profiles have been randomly generated between 20 m/s and 40 m/s and are displayed for each area in Fig. 10, which is a realistic approach in windstorms. It is worth pointing out that the longitudes and latitudes of the buses have been retrieved manually, but the towers have been placed along a line, which implies that all poles are equally affected by the same wind attack angle within a gridded area. Although the length span may affect the vulnerability of the models, as seen in [80], a fixed span of 0.3 km has been used in this study.

a: RESULTS DISCUSSION

A sensitivity analysis has been conducted using the model described in the previous Section and considering the FCs of several articles, leading to seven case studies. The first two consider the FCs obtained from [79] (i.e., a base case and +/− 20 %), in which the tower-line interaction is considered in the first case study and dismissed in the second one, following the values in Figs. 7(a) and 7(b) of [79]. In a similar way, case 3 has taken advantage of the FCs for transmission towers suggested in [76]. Afterwards, the curves shown in Fig. 5 are
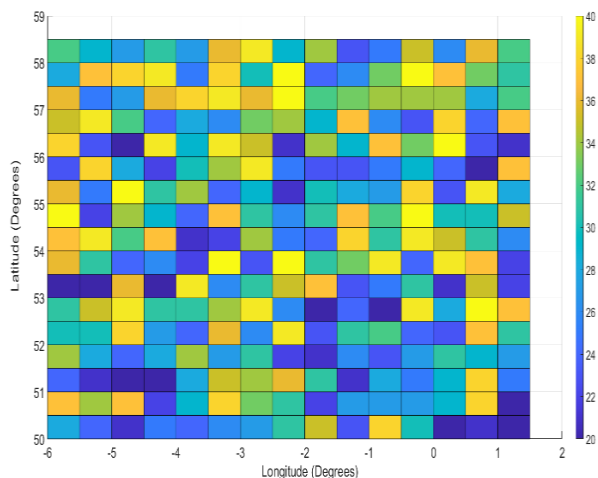
FIGURE 10. Wind-speed values in each area across the GB.

TABLE 2. Data of section VI-A2 for transmission systems.

Case	Ref.	Nº of Vulnerable lines (P_{th})				
		P_{th} 0	P_{th} 0.05	P_{th} 0.1	P_{th} 0.15	P_{th} 0.2
1	[79]	57	51	51	50	50
2	[79]	45	0	0	0	0
3	[76]	48	27	27	27	25
4	[59]	62	45	45	43	40
5	[59]	62	4	4	0	0
6	[59]	62	0	0	0	0
7	[70]	62	7	0	0	0

used to generate three cases, that is, cases 4 through 6, where each one stands for a different level of robustness. It must be said that the FCs used in cases 1 through 3 included both wind speed and angle, whereas cases 4 through 6 are agnostic of the angle. Finally, the empirical curves retrieved from [70] are considered in case 7. The values plotted in Fig. 6 are the failure rate for a given line length, so an exponential distribution has been assumed to obtain probabilities of failure. By utilising the equations in Section VI-A1 and according to the procedure followed in some resilience assessments [25], [28], [34], [54], [59], [63], [120], a threshold value needs to be set to obtain the vulnerable lines. How to establish this threshold is certainly a tradeoff between a conservative scenario with a low value causing a large number of affected lines and large values leading to a fewer number of damaged lines [59]. Thence, five different values have been considered to obtain a variety of scenarios. The results of the sensitivity analysis are summarised in Table 2.

As one can expect, the lower the threshold, the larger the number of lines considered vulnerable. Nevertheless, several differences are observed in Table 2. In particular, the FCs used in cases 1 and 2 belong to the same paper and solely

TABLE 3. Data of section VI-A3 for distribution systems.

Poles and lines	Nº of Poles	Fragility curves (Ref.)	Share of each Pole type (%)
OHL (Wood-C3)	192	[73]	30
OHL (Wood-C5)	152	[73]	23.75
OHL (Wood-C5LA*)	44	[81]	6.25
OHL (Steel)	192	[51]	30
Underground	64	-	10

differ from one another with the interaction between the wires and towers, resulting in a more robust scenario for Case 2. By observing the values in the third column, however, it is seen that such a model provides a similar behaviour for the lowest threshold setting but shows a different performance for the rest of the settings. The narrow differences observed between the curves depicted in Fig. 5 can now be expressed in terms of the number of vulnerable lines.

Therefore, the impact that the FCs have on the resilience assessments can be measured from the results in Table 2. Henceforth, given a threshold of 0.05 p.u., 82 per cent of lines are vulnerable in Case 1, whereas Case 3, with a similar model, gives 43 per cent of vulnerable lines. As observed in Fig. 5, the larger the percentage of robustness, the lower the probability of failure. Additionally, the results of Case 1 are fairly close to those in Case 4, even though the wind attack angle is not considered in the latest one.

3) DISTRIBUTION SYSTEMS

To quantify the impact of the vulnerability model on resilience assessments during windstorms for distribution networks, three case studies were considered using the IEEE 33-bus system. A total length of 2 km has been considered in each line with a span of 100 m between poles, giving a total number of 640 poles. To accurately capture the effects of such deterioration over time, the authors opted for implementing a lognormal distribution with μ and σ of 3.44 and 0.3, respectively. Since the FCs in Section II-A are based on a particular age, the obtained values have been regrouped with sets of ages (i.e., 10/20/40/60/80- years-old and 0/20/40/60 years old, for wood and steel, respectively). The poles have been normally distributed around the age of 30. The FCs used for straight wood poles can be found in [73], the curves used for steel poles are retrieved from [81], whilst the class five bent poles are from [51], respectively. A summary of the features of the third case is included in Table 3. The first case system is uniquely composed of class three wood poles. Secondly, class five wood poles have been added to the previous case.

Thirdly, steel poles are included in the third case in conjunction with wood classes three and five, leading to a casuistry wherein three types of poles are deemed. The wind values used as input to compute the failure probabilities are shown in Fig. 11. This wind profile was recorded in the UK
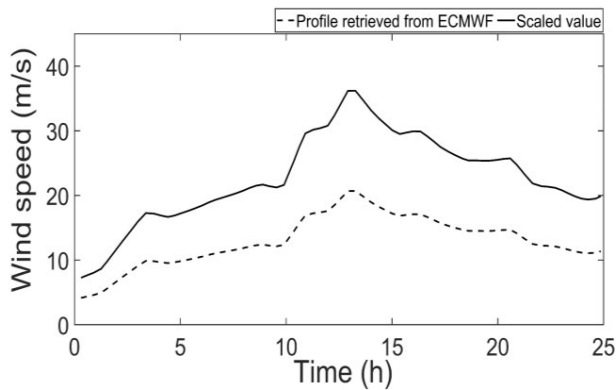
FIGURE 11. 24-hour wind-speed profile retrieved and scaled.

on the 27th of February 2022 during storm EUNICE and has been retrieved from ECMWF [121]. This averaged profile does not exactly match the 3-s wind gust recorded by the UK Met office, as it has been averaged hourly. Consequently, these values have been scaled to match those values with a multiplying factor of 1.75.

a: RESULTS DISCUSSION

This Section aims to compare differences between the number of vulnerable lines obtained between the three cases exposed in Section A.3.

The outcomes of these simulations are displayed in Figs. 12 (a)-(c) over a 24-h period for cases 1 through 3, respectively. Please note that lines are considered out-of-service for the whole assessment since the moment P_{th} is above the established thresholds. It is seen that for low thresholds, the result between cases is the same. Contrarily, slight differences are observed for thresholds larger than 0.05, for instance, there is a difference of four lines between Cases 1 and 3 if the threshold is set to 0.1. Since class 3 wood poles have a higher degree of robustness w.r.t. to those of class five, the number of vulnerable lines is higher after adding the class five wood poles to the configuration of case 1. Moreover, regardless of the vulnerability threshold, comparing Fig. 12 (a) with Fig. 12 (b), differences in many lines can be seen. It is expected that t = 13 is the most unfavourable as the wind profile reaches its peak, yet results vary between the three cases. The largest difference between cases is identified in line 16, where the probabilities of failure are 0.21, 0.77 and 0.56. This notable variation between cases 1 and 3 is attributable to the grid composition, as the number of poles and ages remains the same.

B. RESILIENCE ASSESSMENTS FOR EARTHQUAKES

In this Section, the effects of earthquakes on the distribution poles are scrutinised with different types of FCs. The rest of the distribution network elements, such as substations and protection devices, have been omitted, as no comparison is possible if only one FCs is available. Despite that [85] and [87] use different physical magnitudes as input variables (i.e.,

PGA and SA), those approaches are comparable as have been widely used in resilience assessments. Although there is a slight difference between those two variables in [87], this paper uses the same value for comparison purposes. The approach detailed in [85] considered that a certain value of PGA can cause a certain percentage of unavailability w.r.t the total of lines in the system, irrespective of which element is subject to the largest value. On the other hand, the approach in [87] can be specifically applied to pinpoint a particular line of the grid. Considering the previous description and using the 33-bus test system defined in Section A.2.1, a comparison is performed, assuming that lines 2-23/23-24 and 24-25 of that system are subject to a peak ground acceleration of 0.4 g. Fig. 13 illustrates the following case study. According to the curves obtained from [85] and displayed in Fig. 14, given a PGA of 0.4 g, the probabilities of having a slight and moderate disruption are 0.81 and 0.5, respectively. These two categories of affectation imply four and twelve per cent of affected lines, respectively. If a threshold of 0.05 is considered instead, the moderate damage implies that four lines are vulnerable, but does not conclude which ones.

VII. FACTORS INFLUENCING THE FCs

As can be drawn from the previous sections, the use of FCs leads to different results as the shape of these curves varies upon the nature of the element and event. Purposefully, this Section puts the emphasis on examining the main reasons behind these variations, thus highlighting the influential factors of each typology covered in Section III.

The curves designed for transmission systems against wind events that stem from real observations, such as those in [8], offer high fidelity yet leave the following questions unanswered

- What was the age of the damaged tower?
- When performing the database of events to obtain the FCs, was that fault permanent and, therefore, the tower totally collapsed, or was it a temporary fault instead?
- Did any other factor, such as ice and snow, affect the structure in conjunction with the wind gust?
- What was the angle of the wind in that region?
- Since values are averaged, what was the wind gust value associated with that event?

Secondly, the wind-based FCs obtained from analytical techniques such as the ones in [41] and [42] for transmission systems and [11], [12], and [13] for distribution systems provide answers to some of the previously raised questions but still pose the following concerns

- The external factors, such as objects affecting the line, are very difficult to model and need further exploration.
- The fatigue due to previous events of the same nature has not yet been considered.
- The available FCs for transmission towers against wind events have not considered deterioration over time.
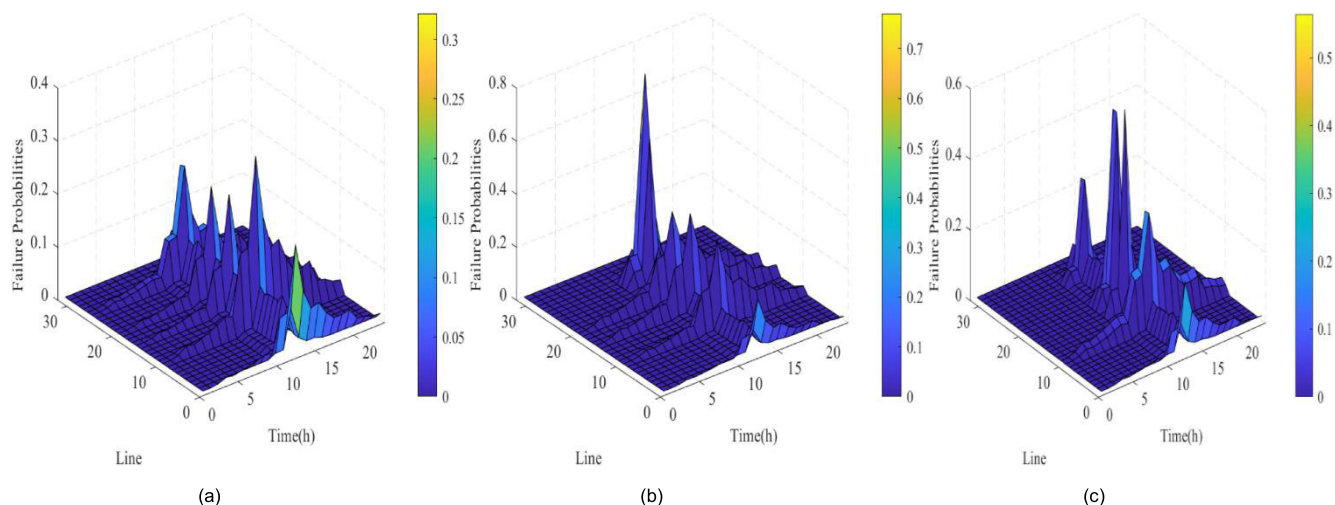
FIGURE 12. Results of the case studies in Section VI-A2 for wind events in distribution networks.
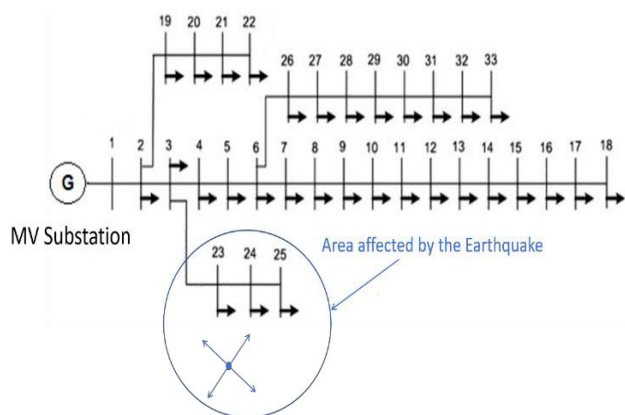

FIGURE 13. Test system used in Section VI-B for earthquakes.
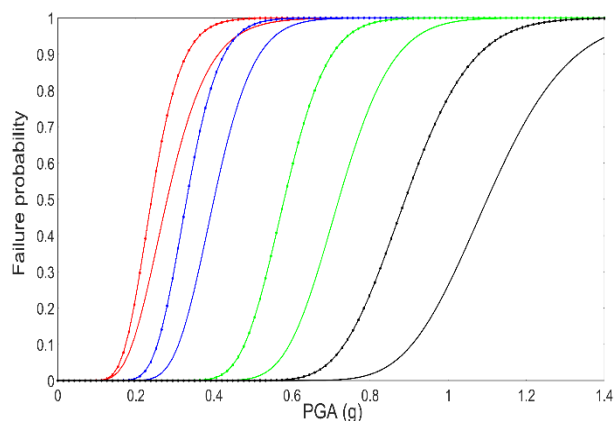

FIGURE 14. FCs retrieved from [85].

- FCs developed for distribution poles dismissed the angle of the wind, which can largely affect the robustness, as seen for the transmission case.

VIII. CONCLUSION AND FUTURE RESEARCH

This paper has reviewed the main typologies of FCs used in the resilience assessments for electrical power systems. The FCs have been divided according to the input variable, which is the physical magnitude associated with each hazard. As a main conclusion, it has been found that some categories, such as wind-based FCs have gained much attention in recent years, and therefore, a large number of curves are available for both transmission and distribution networks. On the contrary, very little has been done regarding categories like flooding and lightning, leaving room for future research.

This paper has also established a relationship between some resilience assessments and the FCs used in each one, thus identifying the most and least used curves in each field. The results provided in Section IV give a clear picture of the number of available research articles for each type of FC and the evolution of the trend over the last 20 years. If each typology of FC is analysed separately, nonetheless, it is clear that despite the huge efforts towards modelling the effects of wildfires, ice storms and lightning on the network components, research is still required. Based on the previous reasoning, the following research lines are suggested for the least developed types of FCs

- Improve the current FCs designed for flooding and expand those curves to different system components and features (e.g., sheltered substations, outdoor equipment in outdoor HV substations, GIS substations, etc.)
- Develop FCs for wildfires with considering reliable physical magnitudes to facilitate the assessment of those events.
- Carry out extensive simulation studies to enhance the performance of FCs for ice storms to achieve a 3-D plot with two main input variables e.g., wind speed and accumulated ice accretion.

This article provides a comprehensive sensitivity analysis in Section VI, which quantifies the impact of different FCs on resilience assessments.

Finally, it is worth highlighting that this research can be a useful tool for power systems engineers and researchers to perform future resilience studies according to each particular type of natural hazard.

REFERENCES

[1] C. Howarth and D. Viner, "Integrating adaptation practice in assessments of climate change science: The case of IPCC Working Group II reports," *Environ. Sci. Policy*, vol. 135, pp. 1–5, Sep. 2022.

[2] S. Dian, P. Cheng, Q. Ye, J. Wu, R. Luo, C. Wang, D. Hui, N. Zhou, D. Zou, Q. Yu, and X. Gong, "Integrating wildfires propagation prediction into early warning of electrical transmission line outages," *IEEE Access*, vol. 7, pp. 27586–27603, 2019.

[3] A. M. Fernandes, A. B. Utkin, and P. Chaves, "Automatic early detection of wildfire smoke with visible light cameras using deep learning and visual explanation," *IEEE Access*, vol. 10, pp. 12814–12828, 2022.

[4] K. van der Geest and R. van den Berg, "Slow-onset events: A review of the evidence from the IPCC Special Reports on Land, Oceans and Cryosphere," *Current Opinion Environ. Sustainability*, vol. 50, pp. 109–120, Jun. 2021.

[5] H. Raoufi, V. Vahidinasab, and K. Mehran, "Power systems resilience metrics: A comprehensive review of challenges and outlook," *Sustainability*, vol. 12, no. 22, p. 9698, Nov. 2020.

[6] *The Exacerbated Effect of Storms Dudley, Eunice and Franklin in the U.K.*, Ambiental Risk Analytics, Brighton, U.K., 2022.

[7] *Hurricanes Harvey and Irma Show U.S. Must Boost Grid Resiliency. Energy Storage Is Doing Just That*, Forbes, Jersey City, NJ, USA. [Online]. Available: https://www.forbes.com/sites/energyinnovation/2017/09/08/hurricanes-harvey-and-irma-show-u-s-must-boost-grid-resiliency-energy-storage-is-doing-just-that/?sh=60aeb7a624c9

[8] J. W. Busby, K. Baker, M. D. Bazilian, A. Q. Gilbert, E. Grubert, V. Rai, J. D. Rhodes, S. Shidore, C. A. Smith, and M. E. Webber, "Cascading risks: Understanding the 2021 winter blackout in Texas," *Energy Res. Social Sci.*, vol. 77, Jul. 2021, Art. no. 102106.

[9] A. Karaer, M. Chen, M. Gazzea, M. Ghorbanzadeh, T. Abichou, R. Arghandeh, and E. E. Ozguven, "Remote sensing-based comparative damage assessment of historical storms and hurricanes in Northwestern Florida," *Int. J. Disaster Risk Reduction*, vol. 72, Apr. 2022, Art. no. 102857.

[10] J. C. Araneda, H. Rudnick, S. Mocarquer, and P. Miquel, "Lessons from the 2010 Chilean earthquake and its impact on electricity supply," in *Proc. Int. Conf. Power Syst. Technol.*, Oct. 2010, pp. 1–7.

[11] S. Ciccotosto, "Costing a natural disaster: An accounting perspective," in *Economic Effects of Natural Disasters*, T. Chaiechi, Ed. New York, NY, USA: Academic, 2021, ch. 15, pp. 225–235.

[12] R. Serrano, M. R. Carvalho, J. C. Araneda, O. Alamos, L. Barroso, D. Bayma, R. Ferreira, and R. Moreno, "Fighting against wildfires in power systems: Lessons and resilient practices from the Chilean and Brazilian experiences," *IEEE Power Energy Mag.*, vol. 20, no. 1, pp. 38–51, Jan. 2022.

[13] A. M. Stankovic et al., "Methods for analysis and quantification of power system resilience," *IEEE Trans. Power Syst.*, vol. 38, no. 5, pp. 4774–4787, Sep. 2023.

[14] M. Abdelmalak and M. Benidris, "Enhancing power system operational resilience against wildfires," *IEEE Trans. Ind. Appl.*, vol. 58, no. 2, pp. 1611–1621, Mar. 2022.

[15] M. H. Amirioun, F. Aminifar, and H. Lesani, "Resilience-oriented proactive management of microgrids against windstorms," *IEEE Trans. Power Syst.*, vol. 33, no. 4, pp. 4275–4284, Jul. 2018.

[16] M. H. Amirioun, F. Aminifar, H. Lesani, and M. Shahidehpour, "Metrics and quantitative framework for assessing microgrid resilience against windstorms," *Int. J. Electr. Power Energy Syst.*, vol. 104, pp. 716–723, Jan. 2019.

[17] J. Bao, X. Wang, Y. Zheng, F. Zhang, X. Huang, P. Sun, and Z. Li, "Resilience-oriented transmission line fragility modeling and real-time risk assessment of thunderstorms," *IEEE Trans. Power Del.*, vol. 36, no. 4, pp. 2363–2373, Aug. 2021.

[18] S. Biswas, M. K. Singh, and V. A. Centeno, "Chance-constrained optimal distribution network partitioning to enhance power grid resilience," *IEEE Access*, vol. 9, pp. 42169–42181, 2021.

[19] P. Cicilio, L. Swartz, B. Vaagensmith, C. Rieger, J. Gentle, T. McJunkin, and E. Cotilla-Sanchez, "Electrical grid resilience framework with uncertainty," *Electric Power Syst. Res.*, vol. 189, Dec. 2020, Art. no. 106801.

[20] N. L. Dehghani, A. B. Jeddi, and A. Shafieezadeh, "Intelligent hurricane resilience enhancement of power distribution systems via deep reinforcement learning," *Appl. Energy*, vol. 285, Mar. 2021, Art. no. 116355.

[21] T. Ding, M. Qu, Z. Wang, B. Chen, C. Chen, and M. Shahidehpour, "Power system resilience enhancement in typhoons using a three-stage day-ahead unit commitment," *IEEE Trans. Smart Grid*, vol. 12, no. 3, pp. 2153–2164, May 2021.

[22] J. Liu, C. Qin, and Y. Yu, "A comprehensive resilience-oriented FLISR method for distribution systems," *IEEE Trans. Smart Grid*, vol. 12, no. 3, pp. 2136–2152, May 2021.

[23] S. Ma, B. Chen, and Z. Wang, "Resilience enhancement strategy for distribution systems under extreme weather events," *IEEE Trans. Smart Grid*, vol. 9, no. 2, pp. 1442–1451, Mar. 2018.

[24] M. Movahednia, A. Kargarian, C. E. Ozdemir, and S. C. Hagen, "Power grid resilience enhancement via protecting electrical substations against flood hazards: A stochastic framework," *IEEE Trans. Ind. Informat.*, vol. 18, no. 3, pp. 2132–2143, Mar. 2022.

[25] A. N. Tari, M. S. Sepasian, and M. T. Kenari, "Resilience assessment and improvement of distribution networks against extreme weather events," *Int. J. Electr. Power Energy Syst.*, vol. 125, Feb. 2021, Art. no. 106414.

[26] M. Nazemi, M. Moeini-Aghtaie, M. Fotuhi-Firuzabad, and P. Dehghanian, "Energy storage planning for enhanced resilience of power distribution networks against earthquakes," *IEEE Trans. Sustain. Energy*, vol. 11, no. 2, pp. 795–806, Apr. 2020.

[27] H. T. Nguyen, J. Muhs, and M. Parvania, "Preparatory operation of automated distribution systems for resilience enhancement of critical loads," *IEEE Trans. Power Del.*, vol. 36, no. 4, pp. 2354–2362, Aug. 2021.

[28] M. Panteli, C. Pickering, S. Wilkinson, R. Dawson, and P. Mancarella, "Power system resilience to extreme weather: Fragility modeling, probabilistic impact assessment, and adaptation measures," *IEEE Trans. Power Syst.*, vol. 32, no. 5, pp. 3747–3757, Sep. 2017.

[29] M. E. Parast, M. H. Nazari, and S. H. Hosseinian, "Resilience improvement of distribution networks using a two-stage stochastic multi-objective programming via microgrids optimal performance," *IEEE Access*, vol. 9, pp. 102930–102952, 2021.

[30] F. P. Marcos, C. M. Domingo, and T. G. S. Román, "Improving distribution network resilience through automation, distributed energy resources, and undergrounding," *Int. J. Electr. Power Energy Syst.*, vol. 141, Oct. 2022, Art. no. 108116.

[31] R. R. Nejad, W. Sun, and A. Golshani, "Distributed restoration for integrated transmission and distribution systems with DERs," *IEEE Trans. Power Syst.*, vol. 34, no. 6, pp. 4964–4973, Nov. 2019.

[32] A. Shahbazi, J. Aghaei, S. Pirouzi, M. Shafie-khah, and J. P. S. Catalão, "Hybrid stochastic/robust optimization model for resilient architecture of distribution networks against extreme weather conditions," *Int. J. Electr. Power Energy Syst.*, vol. 126, Mar. 2021, Art. no. 106576.

[33] S. Skarvelis-Kazakos, M. Van Harte, M. Panteli, E. Ciapessoni, D. Cirio, A. Pitto, R. Moreno, C. Kumar, C. Mak, I. Dobson, C. Challen, M. Papic, and C. Rieger, "Resilience of electric utilities during the COVID-19 pandemic in the framework of the CIGRE definition of power system resilience," *Int. J. Electr. Power Energy Syst.*, vol. 136, Mar. 2022, Art. no. 107703.

[34] L. Souto, J. Yip, W.-Y. Wu, B. Austgen, E. Kutanoglu, J. Hasenbein, Z.-L. Yang, C. W. King, and S. Santoso, "Power system resilience to floods: Modeling, impact assessment, and mid-term mitigation strategies," *Int. J. Electr. Power Energy Syst.*, vol. 135, Feb. 2022, Art. no. 107545.

[35] B. Taheri, A. Safdarian, M. Moeini-Aghtaie, and M. Lehtonen, "Enhancing resilience level of power distribution systems using proactive operational actions," *IEEE Access*, vol. 7, pp. 137378–137389, 2019.

[36] D. N. Trakas and N. D. Hatziargyriou, "Resilience constrained day-ahead unit commitment under extreme weather events," *IEEE Trans. Power Syst.*, vol. 35, no. 2, pp. 1242–1253, Mar. 2020.

[37] K. Utkarsh and F. Ding, "Self-organizing map-based resilience quantification and resilient control of distribution systems under extreme events," *IEEE Trans. Smart Grid*, vol. 13, no. 3, pp. 1923–1937, May 2022.

[38] C. Wang, Y. Hou, F. Qiu, S. Lei, and K. Liu, "Resilience enhancement with sequentially proactive operation strategies," *IEEE Trans. Power Syst.*, vol. 32, no. 4, pp. 2847–2857, Jul. 2017.

[39] Y. Wang, T. Huang, X. Li, J. Tang, Z. Wu, Y. Mo, L. Xue, Y. Zhou, T. Niu, and S. Sun, "A resilience assessment framework for distribution systems under typhoon disasters," *IEEE Access*, vol. 9, pp. 155224–155233, 2021.

[40] M. Yan, X. Ai, M. Shahidehpour, Z. Li, J. Wen, S. Bahramira, and A. Paaso, "Enhancing the transmission grid resilience in ice storms by optimal coordination of power system schedule with pre-positioning and routing of mobile DC de-icing devices," *IEEE Trans. Power Syst.*, vol. 34, no. 4, pp. 2663–2674, Jul. 2019.

[41] N. Zhao, X. Yu, K. Hou, X. Liu, Y. Mu, H. Jia, H. Wang, and H. Wang, "Full-time scale resilience enhancement framework for power transmission system under ice disasters," *Int. J. Electr. Power Energy Syst.*, vol. 126, Mar. 2021, Art. no. 106609.

[42] C. Scawthorn, P. Flores, N. Blais, H. Seligson, E. Tate, S. Chang, E. Mifflin, W. Thomas, J. Murphy, C. Jones, and M. Lawrence, "HAZUS-MH flood loss estimation methodology. II. Damage and loss assessment," *Natural Hazards Rev.*, vol. 7, no. 2, pp. 72–81, May 2006.

[43] M. T. Schultz, B. P. Gouldby, and J. D. Simm, "Beyond the factor of safety: Developing fragility curves to characterize system reliabilty," U.S. Army Corps Eng., Washington, DC, USA, vol. 7, Tech. Rep., 2010.

[44] S. Ahmadi, Y. Saboohi, and A. Vakili, "Frameworks, quantitative indicators, characters, and modeling approaches to analysis of energy system resilience: A review," *Renew. Sustain. Energy Rev.*, vol. 144, Jul. 2021, Art. no. 110988.

[45] J. Jasiūnas, P. D. Lund, and J. Mikkola, "Energy system resilience—A review," *Renew. Sustain. Energy Rev.*, vol. 150, Oct. 2021, Art. no. 111476.

[46] X. Ma, H. Zhou, and Z. Li, "On the resilience of modern power systems: A complex network perspective," *Renew. Sustain. Energy Rev.*, vol. 152, Dec. 2021, Art. no. 111646.

[47] A. Umunnakwe, H. Huang, K. Oikonomou, and K. R. Davis, "Quantitative analysis of power systems resilience: Standardization, categorizations, and challenges," *Renew. Sustain. Energy Rev.*, vol. 149, Oct. 2021, Art. no. 111252.

[48] C. Wang, P. Ju, F. Wu, X. Pan, and Z. Wang, "A systematic review on power system resilience from the perspective of generation, network, and load," *Renew. Sustain. Energy Rev.*, vol. 167, Oct. 2022, Art. no. 112567.

[49] H. Wang and T. Jin, "Prevention and survivability for power distribution resilience: A multi-criteria renewables expansion model," *IEEE Access*, vol. 8, pp. 88422–88433, 2020.

[50] A. Younesi, H. Shayeghi, Z. Wang, P. Siano, A. Mehrizi-Sani, and A. Safari, "Trends in modern power systems resilience: State-of-the-art review," *Renew. Sustain. Energy Rev.*, vol. 162, Jul. 2022, Art. no. 112397.

[51] Y. E. Teoh, A. Alipour, and A. Cancelli, "Probabilistic performance assessment of power distribution infrastructure under wind events," *Eng. Struct.*, vol. 197, Oct. 2019, Art. no. 109199.

[52] D. Alvarado, R. Moreno, A. Street, M. Panteli, P. Mancarella, and G. Strbac, "Co-optimizing substation hardening and transmission expansion against earthquakes: A decision-dependent probability approach," *IEEE Trans. Power Syst.*, vol. 38, no. 3, pp. 2058–2070, May 2023.

[53] M. H. Oboudi, M. Mohammadi, D. N. Trakas, and N. D. Hatziargyriou, "A systematic method for power system hardening to increase resilience against earthquakes," *IEEE Syst. J.*, vol. 15, no. 4, pp. 4970–4979, Dec. 2021.

[54] F. Mohammadi, M. Sahraei-Ardakani, D. N. Trakas, and N. D. Hatziargyriou, "Machine learning assisted stochastic unit commitment during hurricanes with predictable line outages," *IEEE Trans. Power Syst.*, vol. 36, no. 6, pp. 5131–5142, Nov. 2021.

[55] S. Lei, C. Chen, H. Zhou, and Y. Hou, "Routing and scheduling of mobile power sources for distribution system resilience enhancement," *IEEE Trans. Smart Grid*, vol. 10, no. 5, pp. 5650–5662, Sep. 2019.

[56] L. Duchesne, E. Karangelos, A. Sutera, and L. Wehenkel, "Machine learning for ranking day-ahead decisions in the context of short-term operation planning," *Electr. Power Syst. Res.*, vol. 189, Dec. 2020, Art. no. 106548.

[57] M. Noebels, R. Preece, and M. Panteli, "A machine learning approach for real-time selection of preventive actions improving power network resilience," *IET Gener., Transmiss. Distrib.*, vol. 16, no. 1, pp. 181–192, Jan. 2022.

[58] M. Noebels, I. Dobson, and M. Panteli, "Observed acceleration of cascading outages," *IEEE Trans. Power Syst.*, vol. 36, no. 4, pp. 3821–3824, Jul. 2021.

[59] M. Panteli, P. Mancarella, D. N. Trakas, E. Kyriakides, and N. D. Hatziargyriou, "Metrics and quantification of operational and infrastructure resilience in power systems," *IEEE Trans. Power Syst.*, vol. 32, no. 6, pp. 4732–4742, Nov. 2017.

[60] P. Demetriou, M. Asprou, and E. Kyriakides, "A real-time controlled islanding and restoration scheme based on estimated states," *IEEE Trans. Power Syst.*, vol. 34, no. 1, pp. 606–615, Jan. 2019.

[61] A. Hosseinzadeh, A. Zakariazadeh, and S. Ranjbar, "Fast restoration of microgrids using online evaluation metrics considering severe windstorms," *Sustain. Energy, Grids Netw.*, vol. 26, Jun. 2021, Art. no. 100458.

[62] M. Panteli, D. N. Trakas, P. Mancarella, and N. D. Hatziargyriou, "Power systems resilience assessment: Hardening and smart operational enhancement strategies," *Proc. IEEE*, vol. 105, no. 7, pp. 1202–1213, Jul. 2017.

[63] M. Panteli, D. N. Trakas, P. Mancarella, and N. D. Hatziargyriou, "Boosting the power grid resilience to extreme weather events using defensive islanding," *IEEE Trans. Smart Grid*, vol. 7, no. 6, pp. 2913–2922, Nov. 2016.

[64] M. Panteli and P. Mancarella, "Modeling and evaluating the resilience of critical electrical power infrastructure to extreme weather events," *IEEE Syst. J.*, vol. 11, no. 3, pp. 1733–1742, Sep. 2017.

[65] M. Panteli and P. Mancarella, "Influence of extreme weather and climate change on the resilience of power systems: Impacts and possible mitigation strategies," *Electr. Power Syst. Res.*, vol. 127, pp. 259–270, Oct. 2015.

[66] S. Reese, B. A. Bradley, J. Bind, G. Smart, W. Power, and J. Sturman, "Empirical building fragilities from observed damage in the 2009 South Pacific tsunami," *Earth-Sci. Rev.*, vol. 107, nos. 1–2, pp. 156–173, Jul. 2011.

[67] M. S. Khomami, M. T. Kenari, and M. S. Sepasian, "A warning indicator for distribution network to extreme weather events," *Int. Trans. Electr. Energy Syst.*, vol. 29, no. 8, Aug. 2019, Art. no. e12027.

[68] S. Dunn, S. Wilkinson, D. Alderson, H. Fowler, and C. Galasso, "Fragility curves for assessing the resilience of electricity networks constructed from an extensive fault database," *Natural Hazards Rev.*, vol. 19, no. 1, Feb. 2018, Art. no. 04017019.

[69] K. Murray and K. R. W. Bell, "Wind related faults on the GB transmission network," in *Proc. Int. Conf. Probabilistic Methods Appl. Power Syst. (PMAPS)*, Jul. 2014, pp. 1–6.

[70] M. R. Jamieson, G. Strbac, and K. R. W. Bell, "Quantification and visualisation of extreme wind effects on transmission network outage probability and wind generation output," *IET Smart Grid*, vol. 3, no. 2, pp. 112–122, Apr. 2020.

[71] S. A. Zareei, M. Hosseini, and M. Ghafory-Ashtiany, "Seismic failure probability of a 400kV power transformer using analytical fragility curves," *Eng. Failure Anal.*, vol. 70, pp. 273–289, Dec. 2016.

[72] Q. Lu and W. Zhang, "Integrating dynamic Bayesian network and physics-based modeling for risk analysis of a time-dependent power distribution system during hurricanes," *Rel. Eng. Syst. Saf.*, vol. 220, Apr. 2022, Art. no. 108290.

[73] Y. M. Darestani and A. Shafieezadeh, "Multi-dimensional wind fragility functions for wood utility poles," *Eng. Struct.*, vol. 183, pp. 937–948, Mar. 2019.

[74] A. Shafieezadeh, U. P. Onyewuchi, M. M. Begovic, and R. DesRoches, "Age-dependent fragility models of utility wood poles in power distribution networks against extreme wind hazards," *IEEE Trans. Power Del.*, vol. 29, no. 1, pp. 131–139, Feb. 2014.

[75] C. Li, H. Pan, L. Tian, and W. Bi, "Lifetime multi-hazard fragility analysis of transmission towers under earthquake and wind considering wind-induced fatigue effect," *Struct. Saf.*, vol. 99, Nov. 2022, Art. no. 102266.

[76] X. Fu and H.-N. Li, "Uncertainty analysis of the strength capacity and failure path for a transmission tower under a wind load," *J. Wind Eng. Ind. Aerodyn.*, vol. 173, pp. 147–155, Feb. 2018.

[77] X. Fu, H.-N. Li, and G. Li, "Fragility analysis and estimation of collapse status for transmission tower subjected to wind and rain loads," *Struct. Saf.*, vol. 58, pp. 1–10, Jan. 2016.

[78] G. Hou and S. Chen, "Probabilistic modeling of disrupted infrastructures due to fallen trees subjected to extreme winds in urban community," *Natural Hazards*, vol. 102, no. 3, pp. 1323–1350, Jul. 2020.

[79] J. Xue, F. Mohammadi, X. Li, M. Sahraei-Ardakani, G. Ou, and Z. Pu, "Impact of transmission tower-line interaction to the bulk power system during hurricane," *Rel. Eng. Syst. Saf.*, vol. 203, Nov. 2020, Art. no. 107079.

[80] L. Ma, P. Bocchini, and V. Christou, "Fragility models of electrical conductors in power transmission networks subjected to hurricanes," *Struct. Saf.*, vol. 82, Jan. 2020, Art. no. 101890.

[81] S. Lee and Y. Ham, "Probabilistic framework for assessing the vulnerability of power distribution infrastructures under extreme wind conditions," *Sustain. Cities Soc.*, vol. 65, Feb. 2021, Art. no. 102587.

[82] A. M. Salman and Y. Li, "Age-dependent fragility and life-cycle cost analysis of wood and steel power distribution poles subjected to hurricanes," *Struct. Infrastruct. Eng.*, vol. 12, no. 8, pp. 890–903, Aug. 2016.

[83] H. Yuan, W. Zhang, J. Zhu, and A. C. Bagtzoglou, "Resilience assessment of overhead power distribution systems under strong winds for hardening prioritization," *ASCE-ASME J. Risk Uncertainty Eng. Syst., A, Civil Eng.*, vol. 4, no. 4, Dec. 2018, Art. no. 04018037.

[84] Y. M. Darestani, A. Shafieezadeh, and R. DesRoches, "Effects of adjacent spans and correlated failure events on system-level hurricane reliability of power distribution lines," *IEEE Trans. Power Del.*, vol. 33, no. 5, pp. 2305–2314, Oct. 2018.

[85] P. J. Schneider and B. A. Schauer, "HAZUS—Its development and its future," *Natural Hazards Rev.*, vol. 7, no. 2, pp. 40–44, May 2006.

[86] C. Zhao, N. Yu, Y. Oz, J. Wang, and Y. L. Mo, "Seismic fragility analysis of nuclear power plant structure under far-field ground motions," *Eng. Struct.*, vol. 219, Sep. 2020, Art. no. 110890.

[87] A. G. Baghmisheh and M. Mahsuli, "Seismic performance and fragility analysis of power distribution concrete poles," *Soil Dyn. Earthq. Eng.*, vol. 150, Nov. 2021, Art. no. 106909.

[88] M. M. Kassem, S. Beddu, W. Qi Min, C. G. Tan, and F. M. Nazri, "Quantification of the seismic behavior of a steel transmission tower subjected to single and repeated seismic excitations using vulnerability function and collapse margin ratio," *Appl. Sci.*, vol. 12, no. 4, p. 1984, Feb. 2022.

[89] R. Bustamante, G. Mosqueda, and M. Kim, "Enhanced seismic protection system for an emergency diesel generator unit," *Energies*, vol. 15, no. 5, p. 1728, Feb. 2022.

[90] D.-V. Ngo, Y.-J. Kim, and D.-H. Kim, "Seismic fragility assessment of a novel suction bucket foundation for offshore wind turbine under scour condition," *Energies*, vol. 15, no. 2, p. 499, Jan. 2022.

[91] N. H. Dinh, J.-Y. Kim, S.-J. Lee, and K.-K. Choi, "Seismic vulnerability assessment of hybrid mold transformer based on dynamic analyses," *Appl. Sci.*, vol. 9, no. 15, p. 3180, Aug. 2019.

[92] R. Liu, M. Xiong, and D. Tian, "Relationship between damage rate of high-voltage electrical equipment and instrumental seismic intensity," *Adv. Civil Eng.*, vol. 2021, Jan. 2021, Art. no. 5104214.

[93] S. Kitayama, "Procedures and results of assessment of seismic performance of seismically isolated electrical transformers with due consideration for vertical isolation and vertical ground motion effects," Tech. Rep., MCEER-16-0010, 2016.

[94] T. Anagnos, "Development of an electrical substation equipment performance database for evaluation of equipment fragilities," Tech. Rep. 2001/06, 2001.

[95] S. A. Zareei, M. Hosseini, and M. Ghafory-Ashtiany, "Evaluation of power substation equipment seismic vulnerability by multivariate fragility analysis: A case study on a 420 kV circuit breaker," *Soil Dyn. Earthq. Eng.*, vol. 92, pp. 79–94, Jan. 2017.

[96] F. Paolacci and R. Giannini, "Seismic reliability assessment of a high-voltage disconnect switch using an effective fragility analysis," *J. Earthq. Eng.*, vol. 13, no. 2, pp. 217–235, Jan. 2009.

[97] *IEEE Guide for Overhead AC Transmission Line Design*, Standard IEEE Std 1863–2019, 2020, pp. 1–109.

[98] L. Chen, H. Zhang, Q. Wu, and V. Terzija, "A numerical approach for hybrid simulation of power system dynamics considering extreme icing events," *IEEE Trans. Smart Grid*, vol. 9, no. 5, pp. 5038–5046, Sep. 2018.

[99] X. Liu, H. Wang, Q. Sun, and T. Guo, "Research on fault scenario prediction and resilience enhancement strategy of active distribution network under ice disaster," *Int. J. Electr. Power Energy Syst.*, vol. 135, Feb. 2022, Art. no. 107478.

[100] L. Makkonen, "Modeling power line icing in freezing precipitation," *Atmos. Res.*, vol. 46, nos. 1–2, pp. 131–142, Apr. 1998.

[101] L. Yang, Z. Hu, L. Nian, Y. Hao, and L. Li, "Prediction on freezing fraction and collision coefficient in ice accretion model of transmission lines using icing mass growth rate," *IET Gener., Transmiss. Distrib.*, vol. 16, no. 2, pp. 364–375, Jan. 2022.

[102] E. Broström and L. Soder, "Modelling of ice storms for power transmission reliability calculations," Presented at the 15th Power Syst. Comput. Conf. (PSCC), 2005. [Online]. Available: http://urn.kb.se/resolve?urn=urn:nbn:se:kth:diva-52752

[103] A. Kudzys, "Safety of power transmission line structures under wind and ice storms," *Eng. Struct.*, vol. 28, no. 5, pp. 682–689, Apr. 2006.

[104] D. Sánchez-Muñoz, J. L. Domínguez-García, E. Martínez-Gomariz, B. Russo, J. Stevens, and M. Pardo, "Electrical grid risk assessment against flooding in Barcelona and Bristol cities," *Sustainability*, vol. 12, no. 4, p. 1527, Feb. 2020.

[105] W. P. S. Dias and U. Edirisooriya, "Derivation of tsunami damage curves from fragility functions," *Natural Hazards*, vol. 96, no. 3, pp. 1153–1166, Apr. 2019.

[106] S. Jazebi, F. de León, and A. Nelson, "Review of wildfire management techniques—Part I: Causes, prevention, detection, suppression, and data analytics," *IEEE Trans. Power Del.*, vol. 35, no. 1, pp. 430–439, Feb. 2020.

[107] J. L. Rossi, A. Simeoni, B. Moretti, and V. Leroy-Cancellieri, "An analytical model based on radiative heating for the determination of safety distances for wildland fires," *Fire Saf. J.*, vol. 46, no. 8, pp. 520–527, Nov. 2011.

[108] M. Choobineh, B. Ansari, and S. Mohagheghi, "Vulnerability assessment of the power grid against progressing wildfires," *Fire Saf. J.*, vol. 73, pp. 20–28, Apr. 2015.

[109] D. N. Trakas and N. D. Hatziargyriou, "Optimal distribution system operation for enhancing resilience against wildfires," *IEEE Trans. Power Syst.*, vol. 33, no. 2, pp. 2260–2271, Mar. 2018.

[110] S. Mohagheghi and S. Rebennack, "Optimal resilient power grid operation during the course of a progressing wildfire," *Int. J. Electr. Power Energy Syst.*, vol. 73, pp. 843–852, Dec. 2015.

[111] M. Nazemi and P. Dehghanian, "Powering through wildfires: An integrated solution for enhanced safety and resilience in power grids," *IEEE Trans. Ind. Appl.*, vol. 58, no. 3, pp. 4192–4202, May 2022.

[112] R. Moreno, D. N. Trakas, M. Jamieson, M. Panteli, P. Mancarella, G. Strbac, C. Marnay, and N. Hatziargyriou, "Microgrids against wildfires: Distributed energy resources enhance system resilience," *IEEE Power Energy Mag.*, vol. 20, no. 1, pp. 78–89, Jan. 2022.

[113] J. Bao, X. Wang, Y. Zheng, F. Zhang, X. Huang, and P. Sun, "Lightning performance evaluation of transmission line based on data-driven lightning identification, tracking, and analysis," *IEEE Trans. Electromagn. Compat.*, vol. 63, no. 1, pp. 160–171, Feb. 2021.

[114] K. M. J. Murray, "The effect of weather and climate change on the operation of meshed power networks," Ph.D. thesis, Dept. Electron. Elect. Eng., Univ. Strathclyde, Glasgow, U.K., 2017. [Online]. Available: https://stax.strath.ac.uk/concern/theses/vt150j30b

[115] G. F. Kovalev and L. M. Lebedeva, *Reliability of Power Systems*. Cham, Switzerland: Springer, 2019.

[116] *Guidelines for Electrical Transmission Line Structural Loading*.

[117] M. Panteli and P. Mancarella, "The grid: Stronger, bigger, smarter? Presenting a conceptual framework of power system resilience," *IEEE Power Energy Mag.*, vol. 13, no. 3, pp. 58–66, May 2015.

[118] C. Pickering. (2015). *Analytical Fragility Functions for National Grid Transmission Towers*. [Online]. Available: https://gtr.ukri.org/publication/overview?outcomeid=58ca98eb572781.12958897&projectref=EP/I035757/1

[119] K. R. W. Bell and A. N. D. Tleis, "Test system requirements for modelling future power systems," in *Proc. IEEE PES Gen. Meeting*, Jul. 2010, pp. 1–8.

[120] C. Sun, X. Wang, and Y. Zheng, "Data-driven approach for spatiotemporal distribution prediction of fault events in power transmission systems," *Int. J. Electr. Power Energy Syst.*, vol. 113, pp. 726–738, Dec. 2019.

[121] H. Hersbach et al., "The ERA5 global reanalysis," *Quart. J. Royal Meteorolog. Soc.*, vol. 146, no. 730, pp. 1999–2049, 2020.
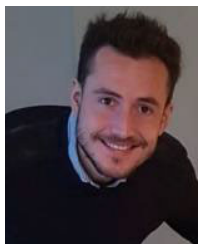
ALEXANDRE SERRANO-FONTOVA (Student Member, IEEE) received the B.S. degree in mechanical engineering from the University of Lleida, Spain, in 2014, the M.S. degree from the European University of Madrid, Madrid, Spain, in 2016, and the Ph.D. degree from the Technical University of Catalonia, Barcelona, Spain, in 2020, as a part of a fully-funded industrial doctorate program in conjunction with a Spanish DSO. He became a part-time Assistant Professor with the Department of Electrical Engineering, Technical University of Catalonia. He received the Award from the Catalan Association of Engineers for the Best Ph.D. Thesis, in 2019. Between 2013 and 2021, he was an Engineer for a Spanish DSO. In 2021, he joined The University of Manchester as a Postdoctoral Researcher to work on advanced data-driven tools to enhance resilience. His research interests include active distribution networks, resilience, and novel protection techniques for distributed energy resources.

ROSA SERRANO (Student Member, IEEE) received the degree in civil engineering of industries and the M.Sc. degree from the Pontifical Catholic University of Chile. She is currently pursuing the Ph.D. degree with the Department of Electrical and Electronic Engineering, The University of Manchester. She is also working on developing tools to improve the resilience of power systems against wildfires. Before starting the Ph.D. degree, she has performed different roles in public and private sectors, including the leading distribution company in Chile, the National Energy Commission, the Chilean Energy Ministry, and the Electricity Network Association in Chile as the Director of Regulation and Studies. She is also the Vice-Chair of IEEE PES Women in Power U.K. and Ireland and the Treasurer of IEEE U.K. and Ireland PES Chapter.

HAIYU LI (Senior Member, IEEE) received the Ph.D. degree in power systems protection and automation from the University of Bath, Bath, U.K., in 1994. Currently, he is a Reader with the Department of Electrical and Electronic Engineering, The University of Manchester, U.K. His expertise is in power systems digitization and automations with emphasis on the applied science for the development of more flexible and sustainable power systems or smart grid. His research interests include active distribution network management systems, distribution networks automations, IEC61850 digital substation automation systems, power systems digitalization, and cyber security. He is a member of IET and a Chartered Engineer in the U.K. He received the IEEE PES Prize Paper Award, in 2017.

ALESSANDRA PARISIO (Senior Member, IEEE) received the Ph.D. degree in automatic control from the University of Sannio, Benevento, Italy. As a Visiting Ph.D. Student, she spent one year with the Swiss Federal Institute of Technology. She was a Postdoctoral Research Fellow with the Automatic Control Laboratory, Royal Institute of Technology, Sweden. She is currently a Lecturer in electrical and electronic engineering with the Faculty of Engineering and Physical Sciences, The University of Manchester, Manchester, U.K. Her research interests include energy management systems under uncertainty, model predictive control, distributed optimization for power systems, the large-scale control and optimization of energy systems, and stochastic constrained control. She received the IEEE PES Outstanding Engineer Award, in January 2021, and the Energy and Buildings Best Paper Award for (for a ten-year period between 2008 and 2017), in January 2019. She is the Vice-Chair of the IFAC Technical Committee 9.3. Control for Smart Cities and an Editor of the *Sustainable Energy, Grids and Networks* journal (Elsevier).

ZHIYU LIAO received the M.Sc. degree in electrical power system engineering from The University of Manchester, U.K., in 2020, where he is currently pursuing the Ph.D. degree with the Department of Electronic and Electrical Engineering. From January 2021 to July 2021, he participated in a project on traveling wave-based transmission line protection for low fault-level networks. His current research interests include power systems resilience, smart grids, and data science.

MATHAIOS PANTELI (Senior Member, IEEE) received the M.Eng. degree in electrical and computer engineering from the Aristotle University of Thessaloniki, Greece, in 2009, and the Ph.D. degree in electrical power engineering from The University of Manchester, U.K., in 2013. He is currently an Assistant Professor with the Department of Electrical and Computer Engineering, University of Cyprus, and an Honorary Lecturer with the Department of Electrical and Electronic Engineering, Imperial College London. His research interests include techno-economic reliability, the resilience and flexibility assessment of future low-carbon energy systems, the grid integration of renewable energy sources, and the integrated modeling and analysis of co-dependent critical infrastructures. He is an IET Chartered Engineer (C.Eng.), the Chair of the CIGRE Working Group C4.47 ''Power System Resilience'' and the CIGRE Cyprus National Committee, and an active member of multiple IEEE working groups.
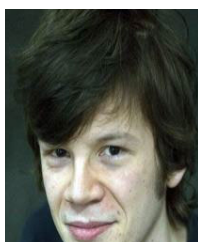
MAGNUS RORY JAMIESON received the dual Ph.D. degree from Imperial College London and the University of Strathclyde. He is currently a researcher in power system resilience and reliability. He specialized in quantifying power system resilience during the course of the Ph.D. degree and he has continued studying the impacts of extreme weather and events on power systems from microgrids to national-scale transmission systems.

• • •